

**Therapeutic potential of mushroom metabolites
against non-structural proteins of SARS-CoV-2**

Project thesis submitted in partial fulfillment of the requirement for
the degree of Bachelor of Technology

In

Bioinformatics

By

HANSIKA DHANJAL(181501)

Under the guidance of

Dr. Raj Kumar



May – 2022

**DEPARTMENT OF BIOTECHNOLOGY AND
BIOINFORMATICS JAYPEE UNIVERSITY OF
INFORMATION TECHNOLOGY WAKNAGHAT, SOLAN,
HIMACHAL PRADESH – 173234.**

TABLE OF CONTENTS

Chapter No.	Topics	Page no.
	Certificate	3
	Declaration	4
	Acknowledgment	5
	List of Figures	6
	List of Tables	8
	Abstract	9
Chapter-1	Introduction	10
Chapter-2	Review of Literature	13
Chapter-3	Materials and Methodology	32
Chapter-4	Results and Discussion	36
Chapter-5	Conclusion	41
	References	42

CERTIFICATE

This is to certify that the work titled “Therapeutic potential of mushroom metabolites against non-structural proteins of SARS-CoV-2”, submitted by “**HANSIKA DHANJAL (181501)**” in partial fulfillment for the award of the degree of B. Tech in Biotechnology of Jaypee University of Information Technology, Solan has been carried out under my supervision. This work has not been submitted partially or wholly to any other University or Institute for the award of this or any other degree or diploma.

Dr. Raj Kumar

Assistant Professor (Grade – II)
Department of Biotechnology and Bioinformatics
Jaypee University of Information Technology (JUIT)
Waknaghat, Solan, India - 173234

Date:

DECLARATION

I hereby declare that the work presented in this report entitled “ **Therapeutic potential of mushroom metabolites against non-structural proteins of SARS-CoV-2**” in partial fulfillment of the requirements for the award of the degree of **Bachelor of Technology** in **Bioinformatics** submitted in the Department of Biotechnology and Bioinformatics, Jaypee University of Information Technology Wanknaghat is an authentic record of my work carried out over a period from August 2021 to May 2022 under the supervision of **Dr. Raj Kumar** (Assistant Professor (Grade – II)) Department of Biotechnology and Bioinformatics.

The matter embodied in the report has not been submitted for the award of any other degree or diploma.

Hansika Dhanjal, 181501

This is to certify that the above statement made by the candidate is true to the best of my knowledge.

Dr. Raj Kumar

Assistant Professor (Grade – II)

Department of Biotechnology and Bioinformatics

Date:

ACKNOWLEDGEMENT

It is indeed a great pleasure to thank all those individuals who have, directly or indirectly, contributed and extended their valuable assistance in the progress and completion of this project.

I thank **Dr. Sudhir Syal**, Head, of the Department of Biotechnology and Bioinformatics, for providing me the opportunity and facilities to carry out the project and for guiding and motivating me whenever required.

I owe my profound gratitude to my project supervisor **Dr. Raj Kumar**, who took a keen interest and guided me all along in my project work titled — **Therapeutic potential of mushroom metabolites against non-structural proteins of SARS-CoV-2**. He provided all the necessary information for carrying out the project. His timely advice, conscientious scrutiny, and scientific approach taught me to work with precision and accuracy and this entity has been a great help to accomplish successful results. I am thankful to him.

It is my privilege to thank my parents for their constant motivation and encouragement. They were always there to provide an affectionate shoulder at odd times or when unsatisfactory results led to frustrations. I am and will always be indebted to their support and care.

Hansika Dhanjal, 181501

LIST OF FIGURES

Figures	Information
Fig 1.	2D structure of Inotodiol
Fig 2.	2D structure of Neosacrodonin A
Fig 3.	2D structure of Cyathatriol
Fig 4.	2D structure of Cyathin-B3
Fig 5.	2D structure of Erinancine A
Fig 6.	2D structure of Lucidadiol
Fig 7.	2D structure of Corpinol
Fig 8.	2D structure of Enokipodin
Fig 9.	2D structure of Ganodermediol
Fig 10.	2D structure of Sarcodonin A
Fig 11.	2D structure of Remdesivir
Fig 12.	2D structure of Nirmatrelvir
Fig 13.	2D structure of Ritonavir
Fig 14.	Macromolecule of 7rv2 protein
Fig 15.	Minimized molecule of 7rv2 protein

Fig 16.	Macromolecule
Fig 17.	H bonds interactions of nsp14 and ritonavir
Fig 18.	2D structure of nsp14 interactions with drug and mushroom metabolite

LIST OF TABLES

Table no.	Subject
Table 1	A brief table about each of the 16 non-structural proteins including their proteins, range, length of each non-structural proteins and their role in the SARS-CoV-2.
Table 2	Docking results of the drugs with the nsp16 macromolecule taken from 7r2v protein molecule.
Table 3	RMSD calculated for experimental and docking pose step by superimposing co-crystal of 7r2v protein with the drugs.
Table 4	Docking results of the secondary mushroom metabolites with the Nsp14 macromolecule taken from 7r2v protein molecule.

Abstract

The novel coronavirus is known to have a number of structural and non-structural proteins that can behave as the therapeutic targets for the antiviral drug designing. There are 4 structural and 16 nonstructural proteins. There are mushrooms that have antiviral properties in them. In this study, nonstructural proteins were explored. Further, nsp14 was used as a drug target for the current study. Medicinal fungi are known to have a several secondary metabolites, which are an important and diversified chemical space of natural goods. 10 such metabolites have been selected and were docked with the non-structural protein 14 for virtual screening. On the other hand 3 FDA approved drugs (Remdesvir, Nirmatrelvir and Ritonavir) were selected as reference compounds for the present study. The binding energy scores of reference inhibitors ref1, ref2, ref3 were -9.5 (ritonavir), -9.4 (remdesivir), -7.8 (nirmatrelvir) kcal/mol. Further compounds exhibited lower binding energy scores and better molecular interactions than the know reference inhibitors. Therefore, we propose that compound ritonavir is a potential inhibitor of SARS-CoV-2 nsp-14 and may be considered for further pre-clinical studies.

CHAPTER-1
INTRODUCTION

The World Health Organization was notified in December 2019 of a pneumonia outbreak in Wuhan, Hubei Province, China, the cause of which was unknown. The severe acute respiratory syndrome coronavirus 2 (SARS-CoV-2) epidemic was declared a public health emergency of international concern by WHO on January 30, 2020. The current coronavirus disease outbreak was formally called Coronavirus Disease-2019 (COVID-19) by the WHO on February 11, 2020, and the virus was termed SARS-CoV-2 by the International Committee on Taxonomy of Viruses (ICTV).^[1]

1.1 SARS-COV-2

SARS-CoV-2 exhibited coronavirus-like features, according to bioinformatic analysis. It's from the beta coronavirus 2B family. Scientists recovered complete genome sequences from five SARS-CoV-2 infected patients in Wuhan early in the pneumonia epidemic. SARS-CoV shares 79.5 percent sequence similarity with these genome sequences^[2]. SARS-CoV-2 is obviously different from SARS-CoV. It is thought to be a new human-infecting beta coronavirus. The entire genome sequence of SARS-CoV-2 and other beta coronavirus genomes were aligned by scientists. The results show that SARS-CoV-2 is most closely related to the bat SARS-like coronavirus strain BatCov RaTG13, with a 96 percent identity. These findings show that SARS-CoV-2 is of bat origin and that it evolved spontaneously from the bat coronavirus RaTG13.

1.1.1 Structure

SARS coronaviruses feature a single-stranded positive-sense RNA that forms a bead-on-the-string arrangement with capsid protein to create the virus particle's protein-ribonucleic helical core^[3]. The viral particle's structural proteins are anchored in a lipid bilayer that surrounds the genetic core. Membrane protein (M), the most prevalent triple-spanning membrane protein required for virus assembly. The smallest of the major structural proteins, envelope (E), is found mostly in vesicle trafficking organelles such as the Golgi and the ER/Golgi interface, and consequently plays a key role in maturation and budding.^[4]

The spike (S) protein creates a trimeric spike that extends from the lipid membrane and

gives the virus a crown-like look, hence the term "corona" virus. Spike protein is required for the virus's infectivity, tissue tropism, and internalization into the host cell. To cause virus replication in the host cell, structural proteins operate in concert with one another.

1.1.2 Proteins

Virus-encoded proteins, like those found in higher-order organisms, perform specialized functions and have both shared and distinct characteristics. Because viruses rely on host mechanisms for replication, similar specializations can also be seen in virus-host interactions, such as varied strategies for manipulating host systems to avoid detection.^[5]

The SARS-CoV-2 genome encodes 28 proteins that have been verified. The major gene, open reading frame 1ab (Orf1ab), is found at the 5' end and encodes the polyproteins PP1ab and PP1a. 16 nonstructural proteins are formed from these polyproteins that are Nsp1 to Nsp16. Genes encoding the four structural proteins (spike [S], envelope [E], membrane [M], and nucleocapsid [N]) as well as eight additional proteins are found in the remaining 3' sequence (Orf3a, Orf3b, Orf6, Orf7a, Orf7b, Orf8, Orf9b, [Orf9c lies outside verified SARS-CoV-2 open reading frame] and Orf10).^[6]

CHAPTER-2

REVIEW OF LITERATURE

2.1 STRUCTURAL PROTEINS

Coronaviruses (CoVs) are members of the Coronaviridae family. These are enclosed viruses having a single-stranded positive RNA genome wrapped within a capsid. The capsid is made up of the nucleocapsid protein N, which is surrounded by a membrane that contains three proteins: the membrane protein (M), the envelope protein (E), and the spike glycoprotein (S), which is involved in binding host receptors, mediating membrane fusion, and virus entry into host cells. Invasion of a host cell is the first phase in SARS-CoV-2 infection, which is mediated by the spike (S) glycoprotein. S1 and S2 are two components of the S protein, which is a glycosylated type I membrane protein. The S protein is found in a trimeric pre-fusion state that is broken into two subunits by a host furin protease. For both SARS-CoV and SARS CoV-2, the N-terminal S1 subunit contained the receptor-binding domain (RBD), which mediated binding to the host cell receptor, notably the angiotensin converting enzyme 2 (ACE2)^[7]. Binding of RBD to ACE2, followed by cleavage of the S2 subunit at a second particular location by the host serine protease TMPRSS2, are required for the dissociation of S1 and S2, which results in conformational changes in S2 that allow for the fusing of viral and host membranes for virus entry. The nucleocapsid protein N plays a multifaceted role in the infection cycle of CoVs. In SARS-CoV, the N protein was reported to bind to, and package the viral RNA into ribonucleoprotein RNP complexes. The packaged RNPs particles are located on the internal face of the viral membrane, forming a separate layer from the envelope proteins M, E and S. Furthermore, RNPs localization could be aided by the interaction between N and the C-terminus of the M protein^[8]. Cryo-ET has recently been used to reveal the architecture of RNPs within newly produced virions. The researchers discovered that RNPs form a 16-nm cylindrical, semi-circular assembly with a favored orientation. Multiple and aligned copies of N proteins generate pillar-shaped densities that are stacked in parallel inside this assembly. The end consequence of this arrangement is the formation of two opposing curved walls.

Through three predicted transmembrane helices, the membrane protein M is lodged in the viral membrane. Its function is to promote the formation of new virions within host cells. Coronavirus M proteins have been demonstrated to oligomerize at the Golgi-endoplasmic

reticulum intermediary compartment membrane and trigger apoptosis. Through contact with the M protein, S, N, and E proteins are recruited. According to the present paradigm, the M protein serves as a scaffolding platform for other structural proteins to recruit and increase membrane curvature during virion budding. Envelope protein E has a single transmembrane domain and can oligomerize. E protein has been shown to generate an ion channel when it interacts with itself via its trans-membrane domain^[9]. The C-terminus of E and M proteins interact to direct E to the Golgi-endoplasmic reticulum intermediary compartment, where viral budding begins.

2.2 NON STRUCTURAL PROTEINS

In the genomic RNA of Severe Acute Respiratory Syndrome, SARS-CoV-2, there are two ORFs, ORF1a and ORF1b, that code for numerous non-structural proteins, NSPs, at the 5' terminal and a few structural proteins, such as envelope protein, membrane proteins, and so on, at the 3' terminal.^[10] The ORF 1ab translated polypeptides are converted into 1-16 NSPs. NSP 1 is a target protein for vaccine development because it is employed by the virus to avoid the host immune system by inhibiting host gene expression^[11]. NSP 2 is not required for viral replication and its function is unknown^[12]. NSPs 2 and 3 combine to create ORF1ab-cleaving proteases. To achieve complete activity of the protein, the structure of NSP 3 shows the presence of RNA-binding domains, SARS Unique Domain, SUD, which contains three subdomains, N-terminal, Middle, and C-terminal domains, and papain like protease, PL-PRO domain^[13]. NSP 3 and NSP 4 work along with other cofactors to cause membrane rearrangement, which is required for viral replication, and the removal of the NSP 3- NSP 4 complex stops viral replication^[14]. NSP 5 is a cysteine-like protease known as 3CL-PRO that processes 11 cleavage sites during replication and has a conserved 3-domain structure and catalytic residues. NSP 6 is engaged in autophagy and creates autophagosomes from the endoplasmic reticulum.

Furthermore, various NSPs have diverse functions in the viral life cycle^[15]. NSP 12 in complex with NSP7 and NSP 8 forms viral replicase machinery, NSP 9 in complex with NSP 8 is involved in RNA replication and virulence, NSP10 - NSP16 complex is required for capping viral mRNA transcripts for efficient translation and evasion of immune surveillance^[16], NSP 14 in complex with its activator NSP 10 is involved in exonuclease activity, NSP 13 is involved in RNA TPase activity, NSP^[17]. Due to selection pressure, adaptive evolution in ORF1a contributes to host shifts or immune evasion, and positive selection drives the evolution of NSPs, shifts, and immune evasion. Despite the fact that most NSPs are orthologous, coronavirus NSP 2 is identical to the bacterial DNA Topoisomerase I and IV required for () strand RNA production, suggesting that NSP 2

could be a therapeutic or vaccine target. Because Nsp16 is required for coronavirus immune evasion, it is particularly crucial in the viral replication cycle. The replication-transcription complex contains Nsp16, a 2'-O-methyltransferase (2'-O-MTase). It performs a vital step in capping transcribed mRNA by mimicking the human protein Cap-specific mRNA (nucleoside-2'-O-)-methyltransferase (CMTr1). Nsp16 enables the transfer of a methyl group from its S-adenosylmethionine (SAM) cofactor to the 2' hydroxyl of viral mRNA's ribose sugar^[18].

Table.1 NSPs and their roles :

S.no.	Protein	Function
1	NSP1	involved in host-range restriction in countering innate host antiviral response and in suppressing induction of apoptosis during early stages of infection to promote viral growth.
2	NSP2	Involved in disruption of intracellular host signaling during SARS-CoV infections.
3	NSP3	It is proposed to facilitate translation of the mRNA transcripts and to suppress host protein synthesis
4	NSP4	Essential role is replication and the assembly of the replicative structures.
5	NSP5	Protease activity
6	NSP6	Generates autophagosomes from the endoplasmic reticulum and is involved in autophagy
7	NSP7	Primer-Independent RNA polymerase Activity

8	NSP8	
9	NSP9	In complex with NSP 8, involved in RNA replication and virulence of virus.
10	NSP10	It is a cofactor for both the 2'O-methyltransferase activity of NSP16, and the N7-guanine-methyltransferase/exoribonuclease activities of NSP14
11	NSP11	Essential for replication
12	NSP12	RNA polymerase/Replicase activity
13	NSP13	Helicase and RNA TPase activity
14	NSP14	Methyl transferase and Exoribonuclease activity
15	NSP15	Uridylate-specific Endoribonuclease activity
16	NSP16	Methyltransferase activity

2.3 NSP14

Understanding the core replication complex of the coronavirus that causes severe acute respiratory syndrome 2 (SARS-CoV-2) is critical for the development of new coronavirus specific antiviral treatments. Nonstructural protein 14 (NSP14), a bifunctional enzyme with an N-terminal 3'-to-5' exoribonuclease (ExoN) and a C-terminal N7-methyltransferase, and its accessory protein, NSP10, are among the proteins necessary for faithful replication of the SARS-CoV-2 genome. The nsp14 limited by the difficulties of manufacturing pure and

large quantities of these key proteins.^[19] Nsp14 protein is an exoribonuclease that is encoded by the coronavirus that causes severe acute respiratory syndrome (SARS-CoV). The coronavirus replicase's bifunctional nsp14 subunit has 3'-to-5' exoribonuclease (ExoN) and guanine-N7-methyltransferase domains. ExoN has been shown to increase genome replication fidelity in the beta coronaviruses MHV and SARS-CoV, likely via facilitating a form of proofreading. ExoN knockout mutants are viable in these viruses, however they have a higher mutation frequency. Surprisingly, we've now proven that similar ExoN knockout mutants of two other beta coronaviruses, MERS-CoV and SARS-CoV-2, are nonviable, implying that ExoN plays a role in their replication as well. This is noteworthy given the close genetic distance between SARS-CoV and SARS-CoV-2, as seen by 95 percent amino acid sequence identity in their nsp14 sequences, for example. Both enzymatic activities of (recombinant) MERS-CoV nsp14 were assessed utilizing recently designed in vitro assays that can be used to further define these essential replicative enzymes and investigate their potential as antiviral therapeutic targets.

2.3.1 NSP14 and NSP10 complex

(SARS)-CoV nsp14 in association with nonstructural protein10 (nsp10), its activator, and functional ligands. ExoN of nsp14 is stabilized and stimulated by one molecule of nsp10 interacting with it. Although the catalytic core of nsp14 ExoN is similar to that of proofreading exonucleases, it is distinguished from homologs by the inclusion of two zinc fingers. Both zinc fingers are required for nsp14 function, according to mutagenesis experiments.^[20]

Nsp10 has several functions in RNA capping, including stimulating exonuclease activity by stabilizing the N-terminal domain. Nsp10 can also form a heterodimer with Nsp16, which has 2'-O-methyltransferase activity specific for 7-methylguanosine-triphosphate-adenosine (m7GppA). In the presence of a methyl group donor, Nsp16 catalyzes the methylation of the nucleotide next to the cap at the 2'-O position after the m7GppA cap is added to the RNA.^[21] Nsp16 activity is activated and the second RNA capping step is completed as a result of this interaction. The structure of the Nsp10-16 complex in SARS-CoV-2 demonstrated a significant degree of similarity between this complex in SARS-CoV-2, SARS-CoV, and MERS-CoV, indicating that it plays a conserved role.^[22]

Surprisingly, Nsp10 has no intrinsic enzymatic activity, despite the fact that it is essential for the function of Nsp14 and Nsp16. Nsp10 most likely performs its job by simply acting as a scaffold for Nsp14 and Nsp16's recruitment to the replication-transcription complex and activation of their specialized activities.^[23] It's yet unknown whether Nsp10 can geographically and temporally coordinate Nsp14 and Nsp16's proof-reading and capping actions, as well as the replication-transcription complex's RNA synthesis timings.^[24]

2.4 Secondary Mushroom Metabolites

1. Inotodiol (PubChem CID: 182264)

Inotodiol is an anti-inflammatory sterol isolated from *Inonotus obliquus*.

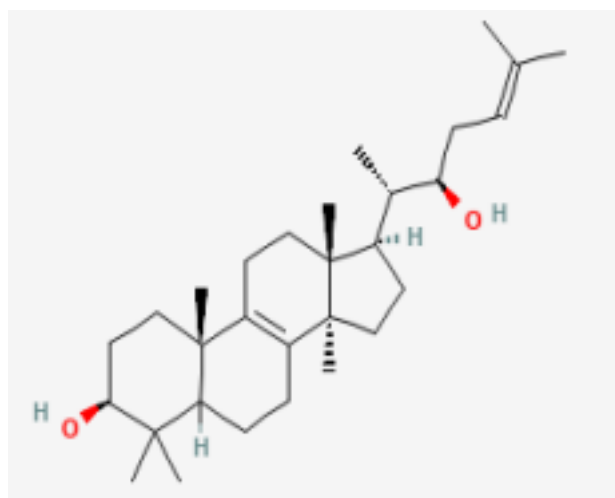


Fig1: 2D structure of Inotodiol

- **Molecular Formula:** C₃₀H₅₀O₂
- **IUPAC names:**
(3S,10S,13R,14R,17R)-17-[(2S,3R)-3-hydroxy-6-methylhept-5-en-2-yl]-4,4,10,13,14-pentamethyl-2,3,5,6,7,11,12,15,16,17-decahydro-1H-cyclopenta[a]phenanthren-3-ol
- **Molecular Weight:** 442.7
- **Hydrogen Bond Donor and Acceptor Count:** 2 and 2

● **Exact Mass:** 442.381080833

● **InChI:**

InChI=1S/C30H50O2/c1-19(2)9-11-24(31)20(3)21-13-17-30(8)23-10-12-25-27(4,5)26(32)15-16-28(25,6)22(23)14-18-29(21,30)7/h9,20-21,24-26,31-32H,10-18H2,1-8H3/t20-,21+,24+,25?,26-,28+,29+,30-/m0/s1

● **InChI Key:** KKWJCGCIAHLFNE-UJHWODAZSA-N

● **Canonical SMILES:**

CC(C1CCC2(C1(CCC3=C2CCC4C3(CCC(C4(C)C)O)C)C)C)C(CC=C(C)C)O

○ **Isomeric SMILES:**

C[C@@H]([C@H]1CC[C@@]2([C@@]1(CCC3=C2CCC4[C@@]3(CC[C@@H](C4(C)C)O)C)C)[C@@H](CC=C(C)C)O

2. Neosarcodonin A (PubChem CID: 101153516)

Neosarcodonin A is an anti-inflammatory cyathane diterpenoids from *Sarcodon scabrosus*.

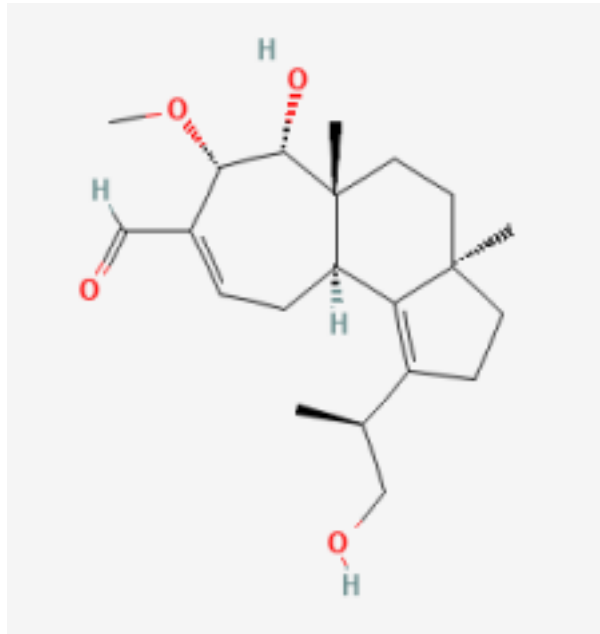


Fig2: 2D structure of Neosarcodonin A

● **Molecular Formula:** C₂₁H₃₂O₄

- **IUPAC names:**

(3aR,5aR,6R,7S,10aR)-6-hydroxy-1-[(2S)-1-hydroxypropan-2-yl]-7-methoxy 3a,5a-dimethyl-2,3,4,5,6,7,10,10a-octahydrocyclohepta[e]indene-8-carbaldehyde ● **Molecular Weight:** 348.5

- **Hydrogen Bond Donor and Acceptor Count:** 2 and 4

- **Exact Mass:** 348.23005950

- **InChI:**InChI=1S/C21H32O4/c1-13(11-22)15-7-8-20(2)9-10-21(3)16(17(15)20)6-5-14(12-23)18(25-4)19(21)24/h5,12-13,16,18-19,22,24H,6-11H2,1-4H3/t13-,16-,18+,19+,20-,21-/m1/s1

- **InChI Key:** KIJQNYNQHIZOJO-MEJVKNBMSA-N

- **Canonical SMILES:**

CC(CO)C1=C2C3CC=C(C(C(C3(CCC2(CC1)C)C)O)OC)C=O

- **Isomeric SMILES:**

C[C@H](CO)C1=C2[C@H]3CC=C([C@@H]([C@@H]([C@@]3(CC[C@@]2(CC1)C)C)O)OC)C=O

3.Cyathatriol (PubChem CID: 101316898)

Cyathatriol is an anti-inflammatory and cytotoxic cyathane diterpenoid from *Cyathus africanus*

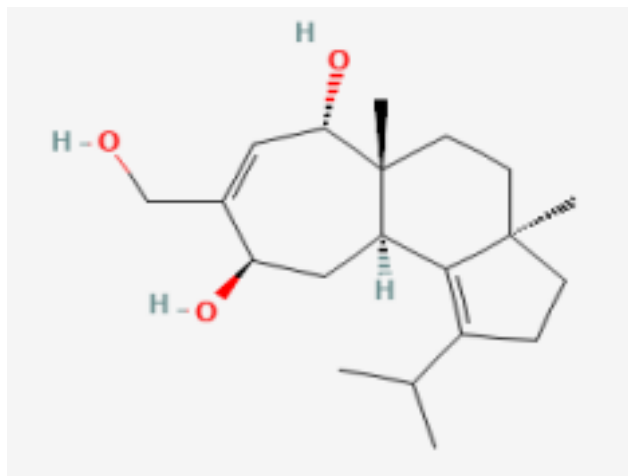


Fig3: 2D structure of Cyathatriol

- **Molecular Formula:** C₂₀H₃₂O₃

- **IUPAC names:** (3aR,5aR,6S,9R,10aR)-8-(hydroxymethyl)-3a,5a-dimethyl-

1- propan-2-yl-2,3,4,5,6,9,10,10a-octahydrocyclohepta[e]indene-6,9-diol

- **Molecular Weight:** 320.5
- **Hydrogen Bond Donor and Acceptor Count:** 3 and 3
- **Exact Mass:** 320.23514488
- **InChI:** InChI=1S/C20H32O3/c1-12(2)14-5-6-19(3)7-8-20(4)15(18(14)19)10-16(22)13(11-21)9-17(20)23/h9,12,15-17,21-23H,5-8,10-11H2,1-4H3/t15-,16-,17+,19-,20-/m1/s1
- **InChI Key:** YQGDZWWLYAMTAU-HPUSYDDDSA-N
- **Canonical SMILES:**
CC(C)C1=C2C3CC(C(=CC(C3(CCC2(CC1)C)C)O)CO)O
- **Isomeric SMILES:**
CC(C)C1=C2[C@H]3C[C@H](C(=C[C@@H]([C@@]3(CC[C@]2(CC1)C)C)O)CO)O

4. Cyathin-B3 (PubChem CID: 102117112)

Cyathin-B3 is an anti-inflammatory diterpenoid from *Cythus Helenae*.

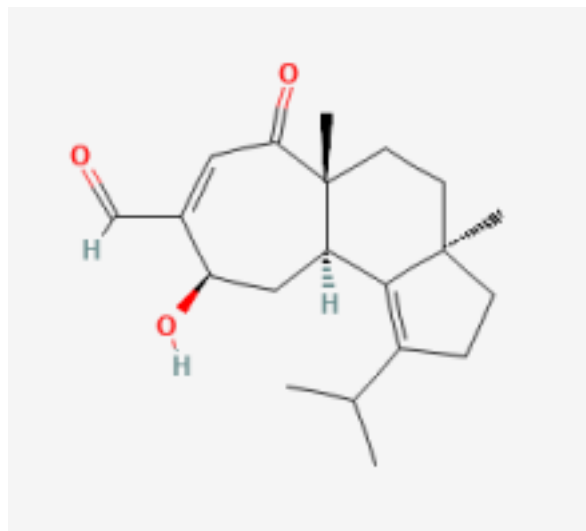


Fig4: 2D structure of Cyathin-B3

- **Molecular Formula:** C₂₀H₂₈O₃
- **IUPAC names:** (3aR,5aR,6S)-6-hydroxy-1-[(2S)-1-hydroxypropan-2-yl]-3a,5a dimethyl-2,3,4,5,6,7-hexahydrocyclohepta[e]indene-8-carbaldehyde
- **Molecular Weight:** 316.4

- **Hydrogen Bond Donor and Acceptor Count:**
- **Exact Mass:** 316.20384475
- **InChI:** InChI=1S/C20H28O3/c1-12(2)14-5-6-19(3)7-8-20(4)15(18(14)19)10-16(22)13(11-21)9-17(20)23/h9,11-12,15-16,22H,5-8,10H2,1-4H3/t15-,16-,19-,20-/m1/s1
- **InChI Key:** HTEKHSBJKOV LAK-XNFNUYLZSA-N
- **Canonical SMILES:**
CC(C)C1=C2C3CC(C(=CC(=O)C3(CCC2(CC1)C)C)C=O)O
- **Isomeric SMILES:**
CC(C)C1=C2[C@H]3C[C@H](C(=CC(=O)[C@@]3(CC[C@]2(CC1)C)C)C=O)O

5. Erinancine A (PubChem CID: 10410568)

Erinancine A is a therapeutic diterpenoid isolated from *Hericium erinaceus*.

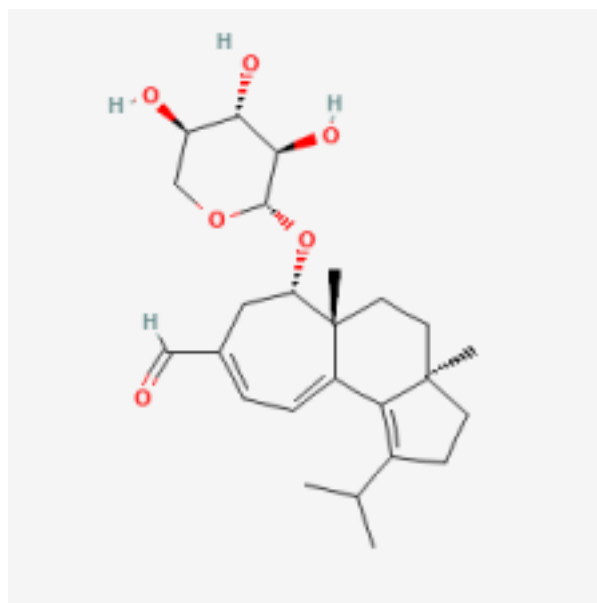


Fig5: 2D structure of Erinancine A

- **Molecular Formula:** C₂₅H₃₆O₆
- **IUPAC names:**
 (3aR,5aR,6S)-3a,5a-dimethyl-1-propan-2-yl-6-[(2S,3R,4S,5R)-3,4,5-

trihydroxyoxan-2-yl]oxy-2,3,4,5,6,7-hexahydrocyclohepta[e]indene-8-carbaldehyde

- **Molecular Weight:** 432.5
- **Hydrogen Bond Donor and Acceptor Count:** 3 and 6
- **Exact Mass:** 432.25118886
- **InChI:** InChI=1S/C25H36O6/c1-14(2)16-7-8-24(3)9-10-25(4)17(20(16)24)6-5-15(12-26)11-19(25)31-23-22(29)21(28)18(27)13-30-23/h5-6,12,14,18-19,21-23,27-29H,7-11,13H2,1-4H3/t18-,19+,21+,22-,23+,24-,25-/m1/s1
- **InChI Key:** LPPCHLAEVDUIIW-NLLUTMDRSA-N
- **Canonical SMILES:**

CC(C)C1=C2C3=CC=C(C(C(C3(CCC2(CC1)C)C)OC4C(C(C(CO4)O)O)O)

C=O ● **Isomeric SMILES:**

CC(C)C1=C2C3=CC=C(C([C@@H]([C@@]3(CC[C@]2(CC1)C)C)O[C@H]4[C@@H]([C@H]([C@@H](CO4)O)O)O)C=O

6. Lucidadiol (PubChem CID:10789991)

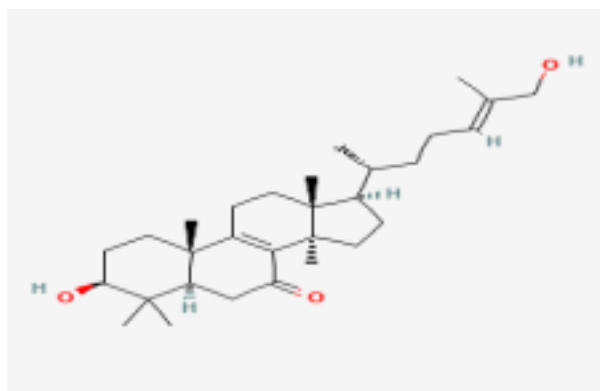


Fig6: 2D structure of Lucidadiol

- **Molecular Formula:** C₃₀H₄₈O₃
- **IUPAC names:**
(3*S*,5*R*,10*S*,13*R*,14*R*,17*R*)-3-hydroxy-17-[(*E*,2*R*)-7-hydroxy-6-methylhept-5-en-2-yl]-4,4,10,13,14-pentamethyl-1,2,3,5,6,11,12,15,16,17-decahydrocyclopenta[a]phenanthren-7-one
- **Molecular Weight:** 456.7
- **Hydrogen Bond Donor and Acceptor Count:** 2,3
- **Exact Mass:**

- **InChI:** InChI=1S/C30H48O3/c1-19(18-31)9-8-10-20(2)21-11-16-30(7)26- 22(12-15-29(21,30)6)28(5)14-13-25(33)27(3,4)24(28)17-23(26)32/h9,20- 21,24-25,31,33H,8,10-18H2,1-7H3/b19-9+/t20-,21-,24+,25+,28-,29-,30+/m1/s1
- **InChI Key:** AZPOACUDFJKUHI-GPEQXWBKSA-N
- **Canonical SMILES:**
CC(CCC=C(C)CO)C1CCC2(C1(CCC3=C2C(=O)CC4C3(CCC(C4(C)C)O)C)C)C
- **Isomeric**
SMILES: C[C@H](CC/C=C(C)/CO)[C@H]1CC[C@@]2([C@@]1(CCC3=C2C(=O)C[C@@H]4[C@@]3(CC[C@H](C4(C)C)O)C)C

7. Corpinol (PubChem CID: 42608175)

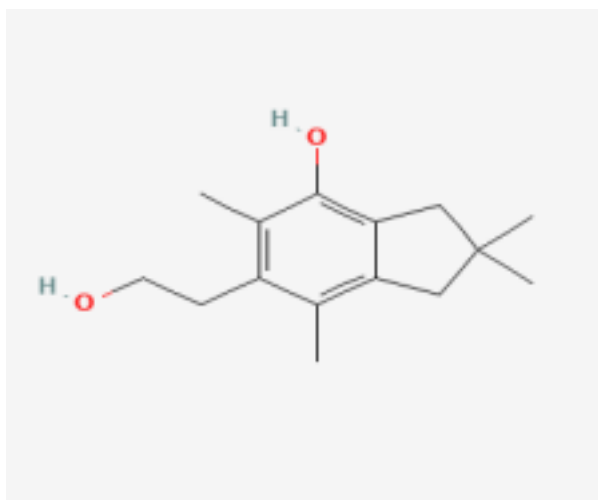


Fig7: 2D structure of Corpinol

- **Molecular Formula:** C₁₅H₂₂O₂
- **IUPAC names:** 6-(2-hydroxyethyl)-2,2,5,7-tetramethyl-1,3-dihydroindene-4-ol
- **Molecular Weight:** 234.33
- **Hydrogen Bond Donor and Acceptor Count:** 2,2
- **Exact Mass:** 234.161979940
- **InChI:** InChI=1S/C15H22O2/c1-9-11(5-6-16)10(2)14(17)13-8-15(3,4)7- 12(9)13/h16-17H,5-8H2,1-4H3
- **InChI Key:** GCMUHPCLXBXQDH-UHFFFAOYSA-N
- **Canonical SMILES:** CC1=C2CC(CC2=C(C(=C1CCO)C)O)(C)C

8. Ganodermediol (PubChem CID: 139586903)

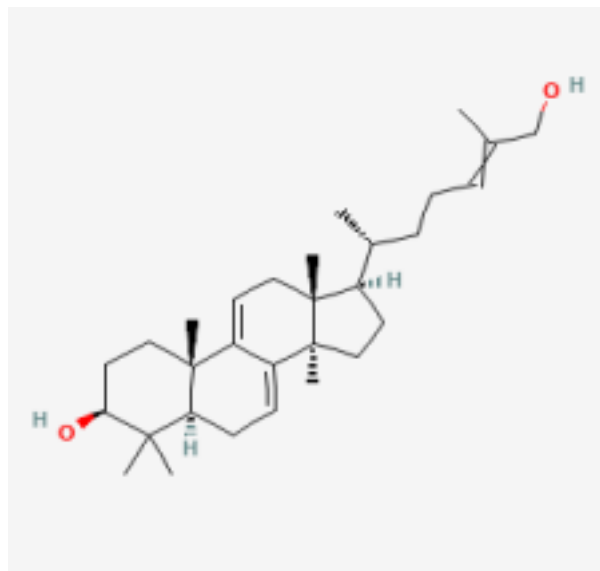


Fig8: 2D structure of Ganodermediol

- **Molecular formula:** C₃₀H₄₈O₂

- **IUPAC NAMES:**

- **MOLECULAR WT:** 440.7

- **HYDROGEN BOND DONOR AND ACCEPTOR COUNT :**

2,2 ● **EXACT MASS :** 440.365430770

- **InChI:** 1S/C₃₀H₄₈O₂/c1-20(19-31)9-8-10-21(2)22-13-17-30(7)24-11-12-25-27(3,4)26(32)15-16-28(25,5)23(24)14-18-29(22,30)6/h9,11,14,21-22,25-26,31-32H,8,10,12-13,15-19H2,1-7H3/t21-,22-,25+,26+,28-,29-,30+/m1/s1 ●

- **InChI key**

- AOXXVRDKZLRGTJ-BQNIITSRSA-N

- **CANONICAL SMILES**

CC(CCC=C(C)CO)C1CCC2(C1(CC=C3C2=CCC4C3(CCC(C4(C)C)O)C)C) ●

- **ISOMERIC SMILES**

C[C@H](CCC=C(C)CO)[C@H]1CC[C@@]2([C@@]1(CC=C3C2=CC[C@@H]4[C@@]3(CC[C@@H](C4(C)C)O)C)C

9.Enokipodin(PubChem CID:10901419)

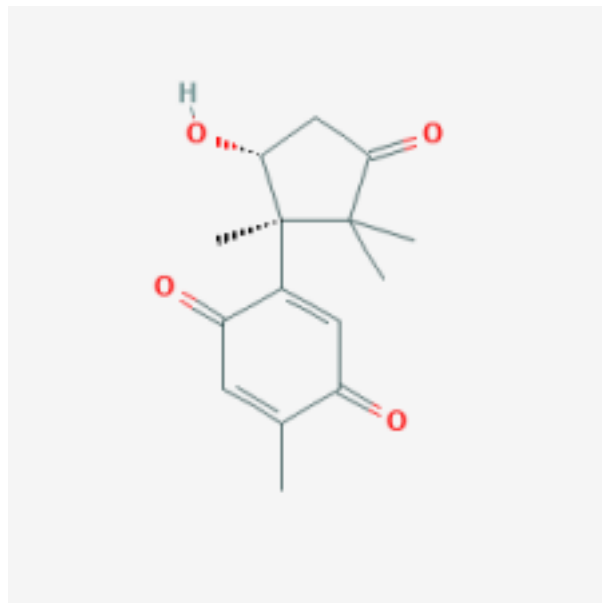


Fig9: 2D structure of Enokipodin

- **MOLECULAR FORMULA** C₁₅H₁₈O₄
- **IUPAC NAME:** 2-[(1*S*,5*R*)-5-hydroxy-1,2,2-trimethyl-3-oxo cyclopentyl]-5-methylcyclohexa-2,5-diene-1,4-dione
- **MOLECULAR Weight:** 262.30
- **HYDROGEN BOND DONOR AND ACCEPTOR COUNT:** 1,4
- **EXACT MASS:** 262.12050905
- **InChI** 1S/C₁₅H₁₈O₄/c1-8-5-11(17)9(6-10(8)16)15(4)13(19)7-12(18)14(15,2)3/h5-6,13,19H,7H2,1-4H3/t13-,15+/m1/s1
- **INChI key**

DBTMIHPJDPGOCQ-HIFRSBDPSA-N

- **CANONICAL SMILES**

CC1=CC(=O)C(=CC1=O)C2(C(CC(=O)C2(C)C)O)C

10.Sarcodonin A (PubChem CID:17747381)

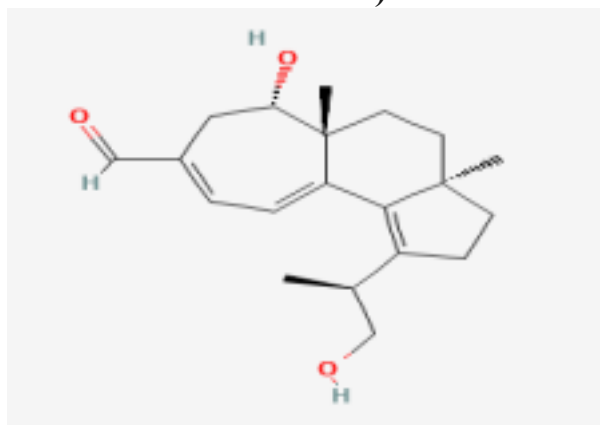


Fig10. 2D structure of Sarcodonin A

- **MOLECULAR FORMULA** C₂₀H₂₈O₃
- **IUPAC NAME:** (3*aR*,5*aR*,6*S*)-6-hydroxy-1-[(2*S*)-1-hydroxypropan-2-yl]-3*a*,5*a*-dimethyl-2,3,4,5,6,7-hexahydrocyclohepta[*e*]indene-8-carbaldehyde ● **MOLECULAR Weight:**316.4
- **HYDROGEN BOND DONOR AND ACCEPTOR COUNT:**
- **EXACT MASS:**
- **InChI** InChI=1S/C₂₀H₂₈O₃/c1-13(11-21)15-6-7-19(2)8-9-20(3)16(18(15)19)5-4-14(12-22)10-17(20)23/h4-5,12-13,17,21,23H,6-11H2,1-3H3/t13-,17+,19-,20-/m1/s1
- **INChI key** HFBBAANNESGPQZ-ISJOWMGUSA
- **CANONICAL SMILES**
CC(CO)C1=C2C3=CC=C(CC(C3(CCC2(CC1)C)C)O)C=O

2.5 FDA approved drugs against SARS-CoV-2

1. REMDESIVIR

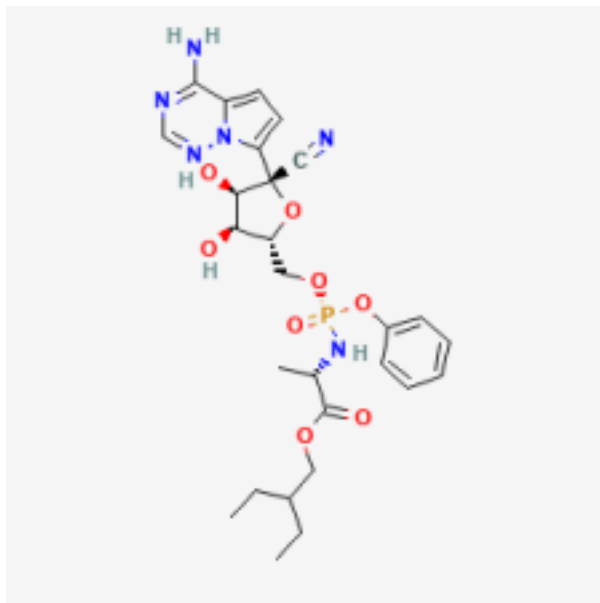


Fig11: 2D structure of Remdesivir

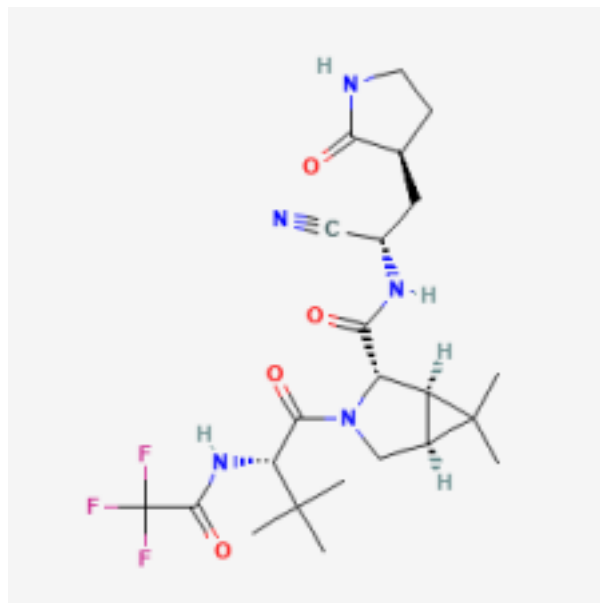
MOLECULAR FORMULA: C₂₇H₃₅N₆O₈P

IUPAC NAME: 2-ethylbutyl (2*S*)-2-[[[(2*R*,3*S*,4*R*,5*R*)-5-(4-aminopyrrolo[2,1-*f*][1,2,4]triazin-7-yl)-5-cyano-3,4-dihydroxyoxolan-2-yl]methoxyphenoxyphosphoryl]amino]propanoate

Remdesivir is an antiviral nucleotide analogue used for therapy of severe novel coronavirus disease 2019 (COVID-19) caused by severe acute respiratory syndrome (SARS) coronavirus 2 (CoV-2) infection.^[25] Remdesivir therapy is given intravenously for 3 to 10 days and is frequently accompanied by transient, reversible mild-to-moderate elevations in serum aminotransferase levels but has been only rarely linked to instances of clinically apparent liver injury, its hepatic effects being overshadowed by the systemic effects of COVID-19.^[26]

MOLECULAR WEIGHT: 602.6

2. NIRMATRELVIR



I Fig12: 2D structure of Nirmatrelvir

MOLECULAR FORMULA: C₂₃H₃₂F₃N₅O₄

IUPAC names:

MOLECULAR WEIGHT: 499.5

Nirmatrelvir is an orally bioavailable inhibitor of the severe acute respiratory syndrome coronavirus-2 (SARS-CoV-2) 3CL protease (3CLpro), with possible antiviral activity against SARS-CoV-2 and other coronaviruses. On oral administration, nirmatrelvir specifically targets and hinders the activity of SARS-CoV-2 3CLpro. This inhibits the proteolytic cleavage of viral polyproteins, thereby inhibiting the formation of viral proteins including helicase, single-stranded-RNA-binding protein, RNA-dependent RNA polymerase, 20-O-ribose methyltransferase, endoribonuclease and exoribonuclease. This prevents viral transcription and replication.^[27]

3. RITONAVIR

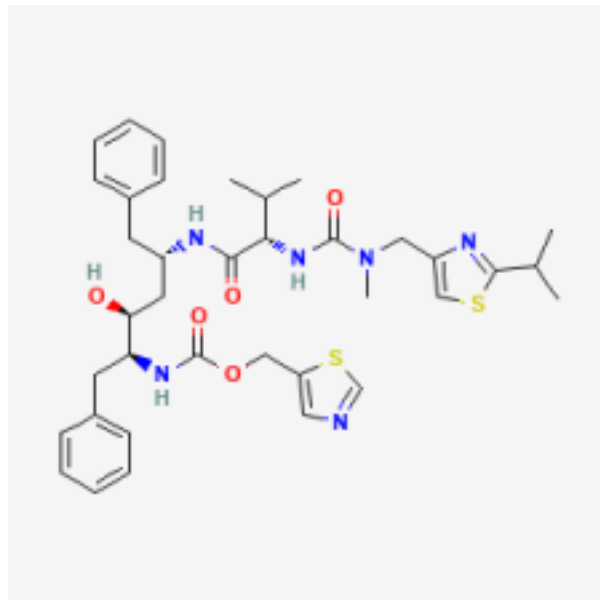


Fig13: 2D structure of Ritonavir

MOLECULAR FORMULA: C₃₇H₄₈N₆O₅S₂

IUPAC names:

1,3-thiazol-5-ylmethyl N-[(2S,3S,5S)-3-hydroxy-5-[[[(2S)-3-methyl-2-[[methyl-[(2-propan-2-yl)-1,3-thiazol-4-yl)methyl]carbonyl]amino]butanoyl]amino]-1,6-diphenylhexan-2-yl]carbamate

MOLECULAR WEIGHT: 720.9

Ritonavir is an antiretroviral protease inhibitor that is widely used in combination with other protease inhibitors in the therapy and prevention of human immunodeficiency virus (HIV) infection and the acquired immunodeficiency syndrome (AIDS). Ritonavir can cause transient and usually asymptomatic elevations in serum aminotransferase levels and, rarely, can lead to clinically apparent acute liver injury.^[28] In HBV or HCV coinfecting patients, highly active antiretroviral therapy with ritonavir may result of an exacerbation of the underlying chronic hepatitis B or C.

CHAPTER -3
MATERIALS AND METHODS

3.1 Predocking

Protein Preparation

1. **Preparation of the target protein for docking using Discovery Studio** - The crystal structure of Nsp14 with PDB ID 7r2v was downloaded from the RCSB protein data bank. The protein was then prepared for pre – docking and structure based calculations by converting it into a macromolecule. By converting the protein into a macromolecule, residues which were not required for further analysis were highlighted and removed and ligand was obtained.



Fig14: Macromolecule of 7rv2 protein

2. **Preparation of the target protein for docking using Chimera** – The obtained ligand was further prepared by removing residues and was minimized using Chimera software which helped in addition and minimization of missing loops, removal of crystal waters and protonation of the ligand through its algorithms.

1. Preparation using PyRx –

The molecule which was minimized and prepared using Chimera was then loaded on PyRx. The molecule was then minimized and converted into a PDBQT ligand. Through Open Babel tool in PyRx, three drug molecules (ritonavir, remdesivir, nirmatrelvir) were loaded. The drug molecules were also minimized and converted and saved into PDBQT ligands.

3. Using autodock vina wizard, ligand and the three drug molecules were loaded for grid preparation. Exhaustiveness for the docking was set at 8. Coordinates of the grid were set as 25 * 25 25.
4. After the docking of the three drug ligands, the macromolecule experimental and docking pose were calculated by superimposing cocrystals of the endoribonuclease of PDB ID 6vww with drug ligands.

3.2 Secondary mushroom metabolites library

Ten Mushroom metabolites were downloaded from PubChem 3D structures of these secondary metaboloids were saved in SDF and PDBQT file format for further docking procedure. A library of the metabolites was prepared. Only those metabolites were chosen in which medicinal therapeutic properties were seen. Two metabolites with antiviral properties (Ganodermediol and Lucidadiol), four metabolites with anti-allergic properties (Cyathatriol, Neosarcodonin, Erinacine, Sarcodonin),

Protein preparation and Grid Preparation for Mushroom Metabolites

1. **Preparation of target protein for docking using discovery studio** – The crystal structure of Nsp14 endoribonuclease with PDB ID 7r2v was downloaded from the RCSB protein data bank. The protein was then prepared for pre – docking and structure based calculations by converting it into macromolecule. By converting that protein into macromolecule, residues which were not required for any further analysis were highlighted and removed and ligand was obtained.

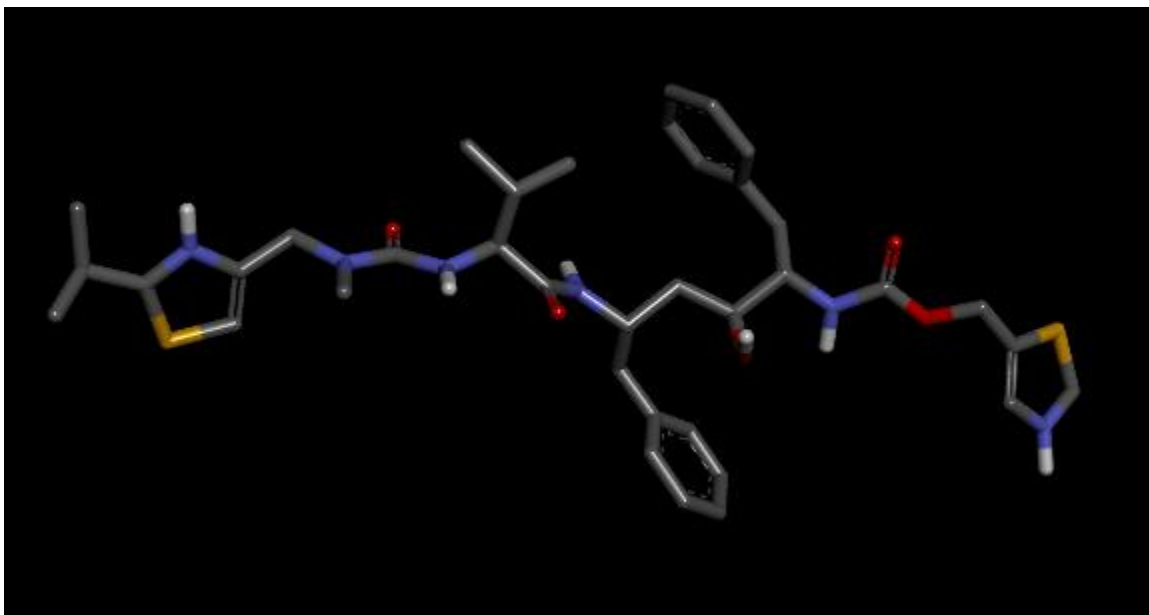


Fig15.Macromolecule converted protein

2. Preparation of target protein for docking using Chimera –

The obtained ligand was further prepared by removing residues and was minimized using Chimera software, which again helped in addition and minimization of missing loops, removal of crystal waters and protonation of ligands through its algorithms.

3. Preparation using PyRx –

The molecule which was prepared and minimized using Chimera was then loaded in PyRx. The molecule was then converted into a PDBQT ligand. Through Open Babel tool in PyRx, ten mushroom metabolites (Inotodiol, Erinacine, Lucidadiol, Enokipodin, Sarcodonin, Coprinol, Neosarcodonin, Cyathatriol, Cyathin, Ganodermediol) were loaded. The terpenoids were also converted and then saved as PDBQT ligands.

4. Using autodock vina wizard, the ligand and the ten secondary mushroom metabolites were loaded for grid preparation. Exhaustiveness for the docking was set at 8. Coordinates of the grid were set as 54.16 33.52 45.03.

CHAPTER -4

RESULTS AND DISCUSSION

1. Virtual screening of the drugs against Nsp14 pre-docking results

After the docking of the 7r2v macromolecule with the three drug ligands the results were as shown in table 2. The ligand of Ritonavir was noticed to have the least binding energy at -9.5 with a root mean square deviation RMSD of 0.0. The three drugs were then superimposed with the co-crystal of 7r2v to complete experimental and docking pose steps. The concluded root mean square deviation RMSD of all three of the drugs was seen to be ≤ 2.0 Å as shown in the table 3.

Molecules	Binding energy
Ritonavir	-9.5
Remdesivir	-9.4
Nirmatrelvir	-7.8

Table 2: Docking results of the drugs with the nsp14 macromolecule taken from 7r2v protein molecule.

Drugs Ligands	RMSD
Ritonavir	1.20
Nirmatrelvir	1.66
Remdesivir	1.49

Table 3: RMSD calculated for experimental and docking pose step by superimposing co crystal of 7r2v protein with the drugs.

1.1 Selection of top lead from drugs and nsp14 docking

Since the ligand of Ritonavir was observed with the least amount of binding energy at -9.5, the compound was chosen as the top lead for further procedure in nsp14 antiviral discovery.

2. Virtual Screening of mushroom metabolites against nsp14

After the affirmation of the experimental and docking pose from the pre-docking results,

the virtual screening of the secondary mushroom metabolites was performed. The ligand dataset of 10 compounds was subjected to virtual screening against the Nsp14 protein target of COVID-19. The virtual screening was performed using an autodock tool implemented in PyRx.

The results of the virtual screening were obtained in a tabular form as shown in table 4. Compounds of Lucidadiol (PubChem CID: 10789991) and Inotodiol(PubChem CID:182264) were noticed to have binding energy less than that of the selected drug Ritonavir, which was observed with a binding energy of -9.5. The ligand of Lucidadiol was observed with a binding energy of -9.1 and RMSD of 0.0 and the ligand of Inotodiol was observed with a binding energy of -9.1 and RMSD of 0.0.

Mushroom Metabolites Ligands	Binding energy	RMSD
Lucidadiol	-9.1	0.0
Inotodiol	-9.1	0.0
Ganodermediol	-8.8	0.0
Cyathin B3	-8.6	0.0
Coprinol	-8.5	0.0
Erinacine A	-8.5	0.0
Enokipodin D	-8.4	0.0
Neosarcodonin A	-8.2	0.0
Sarcodonin A	-7.8	0.0
Cyathatriol	-7.6	0.0

Table 4 - Docking results of the secondary mushroom metabolites with the Nsp14 macromolecule taken from 7r2v protein molecule.

1.1. Selection of top lead from mushroom metabolites.

Since the ligand of Inotodiol was observed with the least amount of binding energy, the compound was chosen as the top lead for nsp14 antiviral discovery.

2. Molecular interaction analysis of top leads from Virtual screening of drugs and mushroom metabolites with Nsp14.

Molecular interaction analysis was performed. This was analyzed through the Biovia Discovery Studio Software. Ligands were loaded and selected and their 2D diagrams were generated. For hydrogen bond interaction conventional hydrogen bonds were visualized and compared as seen in the results given in the figures below.

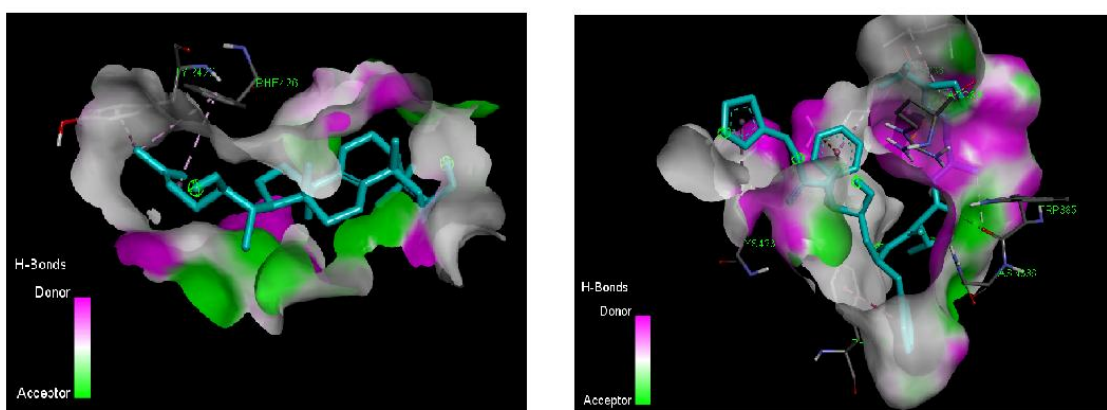


Fig17. H-bonds interactions of nsp14 – ritonavir and nsp14- inotodiol

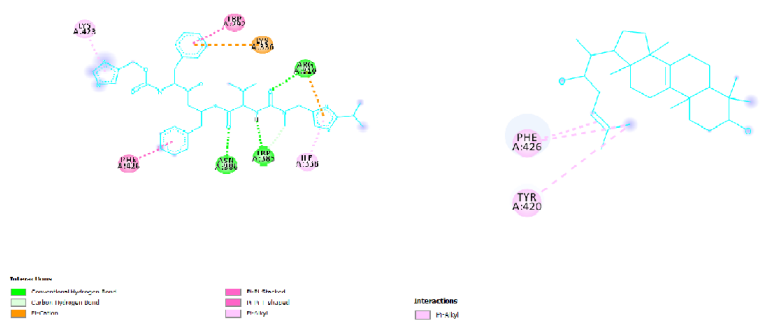


Fig18. 2D structure of nsp14 interactions with drug and inotodiol

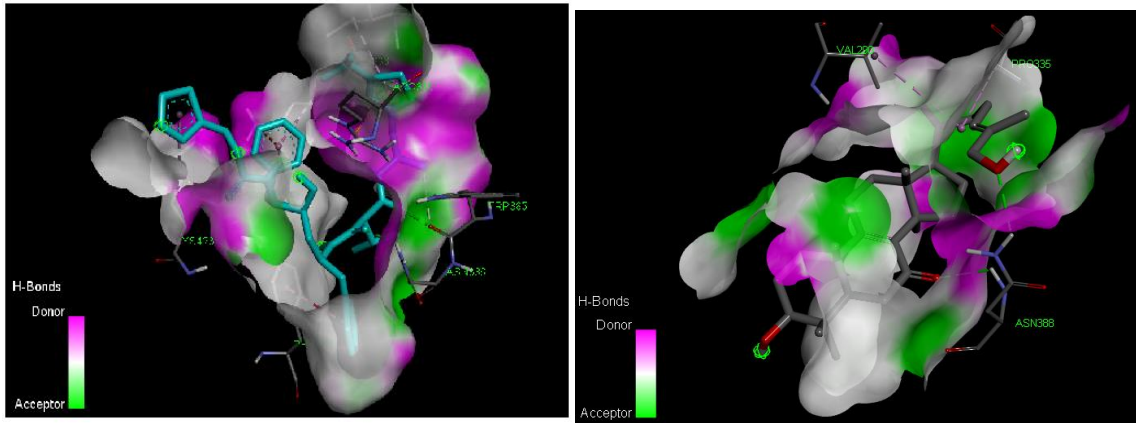


Fig17. H-bonds interactions of nsp14 – ritonavir and nsp14- Lucidadiol

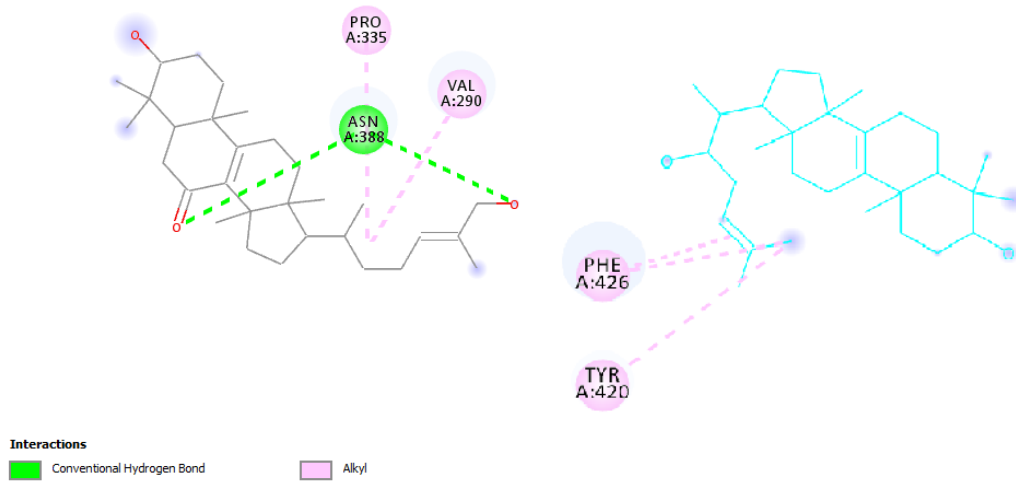


Fig18. 2D structure of nsp14 interactions with drug and Lucidadiol

CONCLUSION

Through the research and experiments conducted above , it can be concluded that the secondary mushroom metabolites, inotodiol (PubChem CID:10789991) that are known to have anti-virals properties and are found to be promising therapeutic targets against SARS-COV-2 targeting specially Nsp14.

This could be concluded because inotodiol and lucidadiol were observed to have the lowest binding energy (-9.1) amongst the 10 secondary mushroom metabolites that were docked with the Nsp14 macromolecule.

REFERENCES

- [1]
P. Krafcikova, J. Silhan, R. Nencka, and E. Boura, “Structural analysis of the SARS-CoV-2 methyltransferase complex involved in RNA cap creation bound to sinefungin,” *Nature Communications*, vol. 11, no. 1, p. 3717, Jul. 2020, doi: 10.1038/s41467-020-17495-9.
- [2]
S. Barage *et al.*, “Identification and characterization of novel RdRp and Nsp15 inhibitors for SARS-COV2 using computational approach,” *Journal of Biomolecular Structure and Dynamics*, vol. 40, no. 6, pp. 2557–2574, Nov. 2020, doi: 10.1080/07391102.2020.1841026.
- [3]
G. Mariano, R. J. Farthing, S. L. M. Lale-Farjat, and J. R. C. Bergeron, “Structural Characterization of SARS-CoV-2: Where We Are, and Where We Need to Be,” *Frontiers in Molecular Biosciences*, vol. 7, p. 605236, 2020, doi: 10.3389/fmolb.2020.605236.
- [4]
B. Cosar *et al.*, “SARS-CoV-2 Mutations and their Viral Variants,” *Cytokine & Growth Factor Reviews*, vol. 63, pp. 10–22, Jul. 2021, doi: 10.1016/j.cytogfr.2021.06.001.
- [5]
M. A. Tortorici and D. Veessler, “Chapter Four - Structural insights into coronavirus entry,” *ScienceDirect*, Jan. 01, 2019. <https://www.sciencedirect.com/science/article/pii/S0065352719300284> (accessed Dec. 13, 2021).
- [6]
A. A. T. Naqvi *et al.*, “Insights into SARS-CoV-2 genome, structure, evolution, pathogenesis and therapies: Structural genomics approach,” *Biochimica et Biophysica Acta. Molecular Basis of Disease*, vol. 1866, no. 10, p. 165878, Oct. 2020, doi: 10.1016/j.bbadis.2020.165878.
- [7]
“Severe acute respiratory syndrome coronavirus 2 isolate Wuhan-Hu-1, complete genome,” *NCBI Nucleotide*, Jul. 2020, Accessed: May 27, 2022. [Online]. Available: https://www.ncbi.nlm.nih.gov/nuccore/NC_045512.2
- [8]
P. V’kovski, A. Kratzel, S. Steiner, H. Stalder, and V. Thiel, “Coronavirus biology and replication: implications for SARS-CoV-2,” *Nature Reviews Microbiology*, vol. 19, pp. 155–170, Oct. 2020, doi: 10.1038/s41579-020-00468-6.
- [9]

M.-Y. Wang, R. Zhao, L.-J. Gao, X.-F. Gao, D.-P. Wang, and J.-M. Cao, “SARS-CoV-2: Structure, Biology, and Structure-Based Therapeutics Development,” *Frontiers in Cellular and Infection Microbiology*, vol. 10, no. 587269, Nov. 2020, doi: 10.3389/fcimb.2020.587269.

[10]

N. Vithani *et al.*, “SARS-CoV-2 Nsp16 activation mechanism and a cryptic pocket with pan coronavirus antiviral potential,” *Biophysical Journal*, vol. 120, no. 14, pp. 2880–2889, Jul. 2021, doi: 10.1016/j.bpj.2021.03.024.

[11]

M. F. Sk, N. A. Jonniya, R. Roy, S. Poddar, and P. Kar, “Computational Investigation of Structural Dynamics of SARS-CoV-2 Methyltransferase-Stimulatory Factor Heterodimer nsp16/nsp10 Bound to the Cofactor SAM,” *Frontiers in Molecular Biosciences*, vol. 7, Nov. 2020, doi: 10.3389/fmolb.2020.590165.

[12]

Y.-Q. Min, Q. Mo, J. Wang, F. Deng, H. Wang, and Y.-J. Ning, “SARS-CoV-2 nsp1: Bioinformatics, Potential Structural and Functional Features, and Implications for Drug/Vaccine Designs,” *Frontiers in Microbiology*, vol. 11, Sep. 2020, doi: 10.3389/fmicb.2020.587317.

[13]

C. Huang, K. G. Lokugamage, J. M. Rozovics, K. Narayanan, B. L. Semler, and S. Makino, “SARS Coronavirus nsp1 Protein Induces Template-Dependent Endonucleolytic Cleavage of mRNAs: Viral mRNAs Are Resistant to nsp1-Induced RNA Cleavage,” *PLoS Pathogens*, vol. 7, no. 12, p. e1002433, Dec. 2011, doi: 10.1371/journal.ppat.1002433.

[14]

C. T. Cornillez-Ty, L. Liao, J. R. Yates, P. Kuhn, and M. J. Buchmeier, “Severe Acute Respiratory Syndrome Coronavirus Nonstructural Protein 2 Interacts with a Host Protein Complex Involved in Mitochondrial Biogenesis and Intracellular Signaling,” *Journal of Virology*, vol. 83, no. 19, pp. 10314–10318, Jul. 2009, doi: 10.1128/jvi.00842-09.

[15]

J. Lei, Y. Kusov, and R. Hilgenfeld, “Nsp3 of coronaviruses: Structures and functions of a large multi-domain protein,” *Antiviral Research*, vol. 149, pp. 58–74, Jan. 2018, doi: 10.1016/j.antiviral.2017.11.001.

[16]

Y. Sakai, K. Kawachi, Y. Terada, H. Omori, Y. Matsuura, and W. Kamitani, “Two-amino acids change in the nsp4 of SARS coronavirus abolishes viral replication,” *Virology*, vol. 510, pp. 165–174, Oct. 2017, doi: 10.1016/j.virol.2017.07.019.

[17]

E. M. Cottam, M. C. Whelband, and T. Wileman, "Coronavirus NSP6 restricts autophagosome expansion," *Autophagy*, vol. 10, no. 8, pp. 1426–1441, Jun. 2014, doi: 10.4161/auto.29309.

[18]

A. J. W. te Velthuis, S. H. E. van den Worm, and E. J. Snijder, "The SARS-coronavirus nsp7+nsp8 complex is a unique multimeric RNA polymerase capable of both de novo initiation and primer extension," *Nucleic Acids Research*, vol. 40, no. 4, pp. 1737–1747, Feb. 2012, doi: 10.1093/nar/gkr893.

[19]

Z. Shi, H. Gao, X. Bai, and H. Yu, "Cryo-EM structure of the human cohesin-NIPBL-DNA complex," *Science*, vol. 368, no. 6498, pp. 1454–1459, May 2020, doi: 10.1126/science.abb0981.

[20]

L. Subissi *et al.*, "One severe acute respiratory syndrome coronavirus protein complex integrates processive RNA polymerase and exonuclease activities," *Proceedings of the National Academy of Sciences*, vol. 111, no. 37, pp. E3900–E3909, Sep. 2014, doi: 10.1073/pnas.1323705111.

[21]

K.-J. Jang, S. Jeong, D. Y. Kang, N. Sp, Y. M. Yang, and D.-E. Kim, "A high ATP concentration enhances the cooperative translocation of the SARS coronavirus helicase nsP13 in the unwinding of duplex RNA," *Scientific Reports*, vol. 10, no. 1, Mar. 2020, doi: 10.1038/s41598-020-61432-1.

[22]

E. Decroly *et al.*, "Crystal Structure and Functional Analysis of the SARS-Coronavirus RNA Cap 2'-O-Methyltransferase nsp10/nsp16 Complex," *PLoS Pathogens*, vol. 7, no. 5, p. e1002059, May 2011, doi: 10.1371/journal.ppat.1002059.

[23]

P. Saini, "COVID-19 pandemic: potential phase III vaccines in development," *The Applied Biology & Chemistry Journal*, pp. 21–33, Sep. 2020, doi: 10.52679/tabcj.2020.0004.

[24]

N. Vithani *et al.*, "SARS-CoV-2 Nsp16 activation mechanism and a cryptic pocket with pan coronavirus antiviral potential," *Biophysical Journal*, vol. 120, no. 14, pp. 2880–2889, Jul. 2021, doi: 10.1016/j.bpj.2021.03.024.

[25]

E. Decroly *et al.*, "Crystal Structure and Functional Analysis of the SARS-Coronavirus RNA Cap 2'-O-Methyltransferase nsp10/nsp16 Complex," *PLoS Pathogens*, vol. 7, no. 5, p. e1002059, May 2011, doi: 10.1371/journal.ppat.1002059.

[26]

PubChem, “Nirmatrelvir,” *pubchem.ncbi.nlm.nih.gov*.
<https://pubchem.ncbi.nlm.nih.gov/compound/155903259> (accessed Apr. 06, 2022).

[27]

PubChem, “Remdesivir,” *pubchem.ncbi.nlm.nih.gov*.
<https://pubchem.ncbi.nlm.nih.gov/compound/Remdesivir> (accessed Apr. 26, 2020).

[28]

PubChem, “Ritonavir,” *pubchem.ncbi.nlm.nih.gov*.
<https://pubchem.ncbi.nlm.nih.gov/compound/392622>